

## An Application of Homogenization Theory to the Coarse-Mesh Nodal Calculation of PWRs

Myung Hyun Kim, Jonghwa Chang, Kap Suk Moon, Chang Kun Lee

Korea Advanced Energy Research Institute

(Received July 16, 1984)

### PWR 소격격자 Nodal 계산에의 균질화 이론 적용

김명현, 장중화, 문갑석, 이창건

한국에너지연구소

(1984. 7. 16 접수)

#### Abstracts

The success of coarse-mesh nodal solution methods provides strong motivation for finding homogenized parameters which, when used in global nodal calculation, will reproduce exactly all average nodal reaction rates for large nodes. Two approximate theories for finding these ideal parameters, namely, simplified equivalence theory and approximate node equivalence theory, are described herein and then applied to the PWR benchmark problem.

Nodal code, ANM<sup>2</sup>, is used for the global calculation as well as for the homogenization calculation. From the comparative analysis, it is recommended that homogenization be carried out only for the unique type of fuel assemblies and for core boundary color-sets. The use of approximate homogenized cross-sections and approximate discontinuity factors predicts nodal powers with maximum error of 0.8% and criticality within 0.1% error relative to the fine-mesh KIDD<sup>2</sup> calculations.

#### 요 약

Nodal method가 소격격자 해석방법의 하나로 정립됨으로써, 계산격자가 비교적 크더라도 각 격자의 평균출력분포를 정확히 계산할 수 있게 하는 균질화변수를 찾는 방법이 중요하게 되었다. 본 연구에서는 simplified equivalence theory와 approximate node equivalence theory의 두가지 근사방법을 가압경수형 원자로 문제에 적용하여 시험하여 보았다.

균질화계산과 노심분석계산 방법으로서 analytic nodal method에 기초를 둔 ANM 코드를 개발하였다. 여러 균질화 방법의 정확성을 KIDD 코드에 의한 reference solution과 비교하여 본 결과, 균질화계산은 핵연료영역에서는 영역별 핵연료집합체 계산으로, baffle과 reflector의 공존 격자영역은 이들을 포함하는 color set 계산으로 수행할 수 있음을 알았다. Approximate node equivalence theory에 입각해서 approximate homogenized cross-section들과 approximate discontinuity factor들의 균질화 변수를 사용하면 출력분포와 임계도가 각각 0.8%, 0.1% 오차 범위내에서 예측되었다.

## I. Introduction

### I.1. Overview

The accurate determination of the behavior of the neutron population is an essential task in the design and analysis of nuclear systems. In thermal reactors, the mean free path length of the neutrons is comparable to the scale of the heterogeneous structure of the assemblies. This causes a strong spatial variation of the neutron spectrum and flux density. Therefore it is not possible to perform a global 2- or 3-dimensional reactor calculations taking into account all these heterogeneity and spectral effects explicitly. In many reactor calculations, detailed pin-cell powers are not directly sought, whereas less detailed quantities such as  $K_{eff}$  and average assembly powers are of primary importance. Consequently, nodal methods which regard the averaged quantities directly as unknowns become to draw keen attention.

Nodal methods generally assume that nodal homogenized parameters (cross-sections and diffusion coefficients) are constant in each node. Thus the application of these methods to realistic reactor problems requires the evaluation of homogenized nodal parameters. Ideally, homogenized parameters are sought, which enable solution of the nodal equations to match (in a node-average sense) a solution obtained with all heterogeneities explicitly modeled. The success of nodal methods depends largely on the accuracy with which these ideal homogenized parameters can be approximated. In this research, homogenization methods for the PWRs are investigated in various aspects and then applied to the benchmark problem.

### I.2. Nodal Homogenization Method

An important advance in nodal homogenization theory was made by Koebke<sup>3)</sup>, who was able to define a formally exact set of homog-

enized parameters. Smith<sup>4)</sup> modified Koebke's theory somewhat by defining a simpler set of exact homogenization parameters and investigated practical ways for approximation of these exact parameters. A homogenized few group neutronic description of the homogenization area is entitled "equivalent," if and when the following postulates are fulfilled:

A : The integral flux and integral reaction rates are conserved in the homogenization area;

B : The integral net currents and integral fluxes are conserved at each interface of this area.

In the exact homogenization theory, additional equivalent parameters (discontinuity factors) are needed to the node weighting averaged cross-sections.

### I.3. Analytic Nodal Method

Earlier nodal models which are based on the 1-group or 1 and a half-group nodal balance equations were incorporated into the FLARE, EPRI-NODE-P/B, TRILUX, PRESTO and SIMULATE codes, and these are widely used by utility companies because of their economic advantages.

In the meantime, advanced nodal methods with stronger theoretical foundations have been devised over the last decade. Advanced nodal methods rely on systematic procedures for the determination of the spatial coupling relations which are needed between node-average fluxes and surface-average currents without relying on empirical adjustments. These methods derive the flux-current spatial coupling equations by decomposing the three-dimensional neutron balance equation in each node into three coupled, one-dimensional equations and solving each one-dimensional equation with an approximate spatial shape assumed for the transverse leakage term. Most nodal methods assume this shape to be quadratic. However, the manner in which

the one-dimensional equations are solved in each node, and the way in which the spatial coupling relations are determined for different nodes, differ among various nodal procedures. These include the flux expansion method, the nodal expansion method, the nodal Green's function method, and the analytic nodal method.

In this research, an analytic nodal method developed by Henry, et al.<sup>4-6)</sup> at MIT are used as a tool of global calculation and node homogenization. The nodal code, ANM<sup>1)</sup>, was developed and benchmarked in comparison with Khalil's thesis<sup>5)</sup>.

The first principle of the equivalence theory is such that the required mathematical structure should be applied in the same manner, generating equivalent parameters or performing succeeding global reactor calculations. For the evaluation of calculation results, however, finite difference method is also used in homogenization procedure and global calculation as an implement for the conventional method solution and reference solution.

## II. Nodal Equivalence Theory

### II.1. Nodal Balance Equations

In the power distribution analysis, fuel depletion is assumed to be a quasi-static process. Exact neutron balance equation can be derived from integration of the time-independent neutron transport equation over all directions  $\hat{\Omega}$ .

$$\begin{aligned} & \nabla \cdot \vec{J}(r, E) + \sum_t(r, E)\phi(r, E) \\ &= \int_0^\infty dE' \{ \sum_{s_0}(r, E' \rightarrow E) \\ &+ \frac{1}{\lambda} M(r, E' \rightarrow E) \} \phi(r, E) \end{aligned} \quad (2.1)$$

where

$$\begin{aligned} M(r, E' \rightarrow E) &\equiv \sum_i \chi^i(E) \nu^i \sum_j^j(r, E) \\ \sum_{s_0}(r, E' \rightarrow E) &\equiv \frac{1}{2} \int_{-1}^1 d\mu_0 \sum_s(r, E' \rightarrow E, \mu_0) \end{aligned}$$

An exact balance equation in node variables can be obtained by integrating Eq. 2.1. over a

nodal volume  $V_{ijk}$  and an energy range  $\Delta E_g$ .

$$\begin{aligned} & h_y^i h_z^k (\bar{J}_{gijk}^{x+} - \bar{J}_{gijk}^{x-}) + h_x^i h_z^k (\bar{J}_{gijk}^{y+} - \bar{J}_{gijk}^{y-}) \\ &+ h_x^i h_y^j (\bar{J}_{gijk}^{z+} - \bar{J}_{gijk}^{z-}) + V_{ijk} \sum_{\Delta g'ijk} \bar{\phi}_{g'ijk} \\ &= V_{ijk} \sum_{g'=1}^G (\sum_{gg'ijk} + \frac{1}{\lambda} M_{gg'ijk}) \bar{\phi}_{g'ijk} \end{aligned} \quad (2.2)$$

where

$$h_x^i \equiv x_{i+1} - x_i$$

$$h_y^j \equiv y_{j+1} - y_j$$

$$h_z^k \equiv z_{k+1} - z_k$$

$$V_{ijk} \equiv h_x^i h_y^j h_z^k$$

$$\bar{\phi}_{gijk} \equiv \frac{1}{V_{ijk}} \int_V d^3r \phi_g(r)$$

$$\phi_g(r) \equiv \int_{\Delta E_g} dE \phi(r, E)$$

$$\bar{J}_{gijk}^{x\pm} \equiv \bar{J}_{gijk}^x(x_{i\pm})$$

$$\begin{aligned} \bar{J}_{gijk}^x(x) &\equiv \frac{1}{h_y^j h_z^k} \int_{y_i}^{y_{j+1}} dy \int_{z_k}^{z_{k+1}} dz \times \\ & \int_{\Delta E_g} dE \vec{J}(r, E) \end{aligned}$$

Heterogeneous, flux-weighted, node-volume-averaged cross sections are defined as

$$\sum_{\alpha g'ijk}^{het} = \frac{\int_{V_{ijk}} d^3r \sum_{\alpha g}(\tau) \phi_g(\tau)}{\bar{\phi}_{gijk} V_{ijk}} \quad (2.3)$$

If the heterogeneous nodes are ideally characterized by the constant-homogenized cross-sections in each node  $(i, j, k)$  and energy range  $\Delta E_g$ , neutron balance equation for homogenized problem are thus

$$\begin{aligned} & \nabla \cdot \vec{J}_g^{hom}(r) + \sum_{ig'ijk}^{hom} \phi_{g'}^{hom}(r) \\ &= \sum_{g'=1}^G [\sum_{gg'ijk}^{hom} + \frac{1}{\lambda_{hom}} M_{gg'ijk}^{hom}] \phi_{g'}^{hom}(r) \end{aligned} \quad (2.4)$$

This equation can also be integrated over a node  $(i, j, k)$  into a homogenized nodal balance equation.

$$\begin{aligned} & h_y^i h_z^k (\bar{J}_{gijk}^{x+,hom} - \bar{J}_{gijk}^{x-,hom}) \\ &+ h_x^i h_z^k (\bar{J}_{gijk}^{y+,hom} - \bar{J}_{gijk}^{y-,hom}) \\ &+ h_x^i h_y^j (\bar{J}_{gijk}^{z+,hom} - \bar{J}_{gijk}^{z-,hom}) \end{aligned}$$

$$\begin{aligned}
 &+ V_{ijk} \sum_{l \in G} \bar{\phi}_{gijk}^{hom} \\
 &= V_{ijk} \sum_{g' \in G} \left( \sum_{gg' \in G} \bar{\phi}_{g'ijk}^{hom} + \frac{1}{\lambda^{hom}} M_{gg'ijk}^{hom} \right) \phi_{gijk}^{hom} \quad (2.5)
 \end{aligned}$$

where  $\phi_{gijk}^{hom}$  and  $\bar{J}_{gijk}^{u\pm, hom}$  are defined in complete analogy with their heterogeneous counterparts as Equation (2.2).

The homogenized cross-sections are valid as exact nodal equivalence parameters and the equivalence between the homogenized problem, Eq. 2.5, and the heterogeneous (exact) problem, Eq. 2.2, is conserved if the following equivalence conditions are satisfied.

$$\lambda^{hom} = \lambda \quad (2.6a)$$

$$\sum_{\alpha gijk}^{hom} \phi_{gijk}^{hom} = \sum_{\alpha gijk} \phi_{gijk} \quad (2.6b)$$

$$\bar{J}_{gijk}^{u\pm, hom} = \bar{J}_{gijk}^{u\pm} \quad (2.6c)$$

These requirements are extremely difficult to be satisfied. For example, the value of  $\sum_{\alpha g}^{hom}$  in Eq. 2.6b requires knowledge not only of heterogeneous reaction rates, but also of information on the homogenized flux distribution that results from the use of the  $\sum_{\alpha g}^{hom}$ . Thus the calculation of these homogenized constants is a nonlinear process.

Solution of the homogenized nodal balance equation, Eq. 2.5, requires a prerequisite that additional equations relating the node-average fluxes  $\phi_g^{hom}$  and the face-average currents  $\bar{J}_g^{hom}$  be derived. In the nodal diffusion theory model, Fick's law is assumed, i.e.,

$$\bar{J}_{gijk}^{hom}(x) = -D_{gijk}^{hom} \frac{d}{dx} \bar{\phi}_{gijk}^{hom}(x) \quad (2.7)$$

where

$$\bar{\phi}_{gijk}^{hom}(x) \equiv \frac{1}{h_y^j h_z^k} \int_{y_j}^{y_{j+1}} dy \int_{z_k}^{z_{k+1}} dz \phi_g(r) \quad (2.8)$$

and the diffusion coefficient  $D_{hom}^g$  is spatially constant in each node.

For direction  $x$  and node  $(i, j, k)$ , the 1-D equation for the homogenized flux may thus be written

$$-D_{gijk}^{hom} \frac{d^2}{dx^2} \bar{\phi}_{gijk}^{X, hom}(x) + \sum_{l \in G} \bar{\phi}_{gijk}^{X, hom}(x) \quad (2.9)$$

$$- \sum_{g' \in G} \left( \sum_{gg' \in G} \bar{\phi}_{g'ijk}^{hom} + \frac{1}{\lambda^{hom}} M_{gg'ijk}^{hom} \right) \bar{\phi}_{gijk}^{X, hom}(x)$$

$$= -S_{gijk}^{y_1 z_1, hom}(x)$$

where

$$S_{gijk}^{y_1 z_1}(x) \equiv \frac{1}{h_y^j} L_{gijk}^y(x) + \frac{1}{h_z^k} L_{gijk}^z(x) \quad (2.10)$$

$$L_{gijk}^y(x) \equiv \frac{1}{h_z^k} \int_{y_j}^{y_{j+1}} dy \int_{z_k}^{z_{k+1}} dx \frac{\partial}{\partial y} J_g^y(r) \quad (2.11)$$

### II.2. Approximate Nodal Equivalence Theory

A practical homogenization method called the approximate homogenization method was developed by Smith<sup>4)</sup>. For each unique assembly type, a relatively inexpensive heterogeneous assembly eigenvalue calculation with zero-net-current boundary conditions yields a heterogeneous assembly flux,  $\phi_g^{het}(x, y, z)$ . With this flux, approximate homogenized cross-sections and diffusion coefficients (AXS) can be calculated by usual flux weighting techniques.

Even if these AXSs are exactly same to the reference heterogeneous values, the requirements for Eq. 2.6 will not be satisfied. Nodal diffusion equations will fail to yield a solution such that the face-averaged currents are correctly matched. Thus nodal equivalence model permits the flux to be discontinuous across each node face by defining two additional homogenization parameters per direction per group. These additional parameters are called "discontinuity factors". Approximate discontinuity factors (ADF) which are obtained from the individual assembly calculation are defined as follows:

$$ADF_{gijk}^{x+} = \frac{\phi_{gijk}^{x, het}(x_{i+1})}{\phi_{gijk}^{x, hom}(x_{i+1})} \quad (2.12)$$

$$ADF_{gijk}^{x-} = \frac{\phi_{gijk}^{x, het}(x_i)}{\phi_{gijk}^{x, hom}(x_i)} \quad (2.13)$$

The numerators of these equations are found immediately by calculating the surface average of the heterogeneous assembly flux which is

$$\phi_{gijk}^{x,het}(x_i) = \frac{1}{h_y^j h_z^k} \int_{y_i}^{y_i+1} dy \int_{z_k}^{z_k+1} dz \phi_{gijk}^{x,het}(x_i, y, z) \quad (2.14)$$

However, the denominators, surface-average homogenized assembly fluxes, must be calculated in a reliable nodal method which is consistent with global calculation method. These denominators in the analytic nodal method applied in this research are given in matrix form.

$$\begin{aligned} [\phi_{gijk}^{x,het}(x_i)] &= [A_{ijk}^x][J_{ijk}^{x,hom}(x_i)] \\ &+ [B_{ijk}^x][\phi_{ijk}^{hom}] - [F_{ijk}^x][S_{i-1,j,k}^{x,hom}] \\ &- [G_{ijk}^x][S_{i,j,k}^{x,hom}] - [H_{ijk}^x][S_{i+1,j,k}^{x,hom}] \quad (2.15) \end{aligned}$$

where

$$\begin{aligned} [F_{ijk}^x] &= [C_{ijk}^x]a_i^- + [D_{ijk}^x]b_i^- + [E_{ijk}^x]C_i^- \\ [G_{ijk}^x] &= [C_{ijk}^x](1-a_i^- - a_i^+) \\ &+ [D_{ijk}^x](-b_i^- - b_i^+) + [E_{ijk}^x](-C_i^- - C_i^+) \\ [H_{ijk}^x] &= [C_{ijk}^x]a_i^+ + [D_{ijk}^x]b_i^+ + [E_{ijk}^x]C_i^+ \end{aligned}$$

Five matrices in Equation 2.15 are defined in the reference (6). They depend only on the homogenized nodal cross-sections, mesh spacings and  $\lambda^{hom}$ . The only approximation used in the derivation of Eq. 2.15 is that the transverse leakage term in Eq. 2.9 is approximated by a function of average transverse leakages of three nodes with quadratic polynomials of  $x$ .

Using this Equation 2.15, denominators of Eq. 2.12 and 2.13 can be calculated. By virtue of this calculation, the proper interface conditions imposed on the homogenized fluxes can be written as

$$ADF_{g^{i-1,j,k}}^{x,+} \phi_{g^{i-1,j,k}}^{x,hom}(x_i) = ADF_{g^{i,j,k}}^{x,-} \phi_{g^{i,j,k}}^{x,hom}(x_i) \quad (2.16)$$

When node homogenization calculation is performed for the fuel assemblies, the homogeneous flux is spatially flat from Eq. 2.15 and thus

$$\phi_{gijk}^{x,hom}(x_i) = \phi_{gijk}^{x,hom}(x_{i+1}) = \phi_{gijk}^{hom} = \phi_{gijk}^{het} \quad (2.17)$$

Therefore, the assemblywise ADF can be expressed as

$$ADF_{gijk}^{x,+} = \phi_{gijk}^{x,het}(x_{i+1}) / \phi_{gijk}^{het} \quad (2.18)$$

and

$$ADF_{gijk}^{x,-} = \phi_{gijk}^{x,het}(x_i) / \phi_{gijk}^{het} \quad (2.19)$$

### II.3. Simplified Equivalence Method

The simplified equivalence theory<sup>3)</sup> is an approximation to the exact equivalence theory<sup>5)</sup>. In this approximation, single heterogeneity factor is introduced as simplified equivalent parameters ( $SE$ ).

$$SE_{gijk}^x = \frac{\phi_{gijk}^{x,het}(x_{i+1})}{\phi_{gijk}^{x,hom}(x_{i+1})} = \frac{\phi_{gijk}^{x,het}(x_i)}{\phi_{gijk}^{x,hom}(x_i)} \quad (2.20)$$

This flux ratio is postulated to be equal on opposite sides of the homogenized area. Therefore, Eq. 2.16 is replaced as

$$SE_{g^{i-1,j,k}}^{x,+} \phi_{g^{i-1,j,k}}^{x,hom}(x_i) = SE_{g^{i,j,k}}^{x,-} \phi_{g^{i,j,k}}^{x,hom}(x_i) \quad (2.21)$$

It is assumed that only one pair of equivalent parameters ( $D_g^{hom}$ ,  $SE_g$ ) is sufficient to describe the neutronic interaction of an homogenization area for all spatial directions.

If the equivalent cross-section library is divided by this  $SE$ -parameters, simplified equivalent cross-section library is produced.

$$\sum_{\alpha gijk}^{SE} = \sum_{\alpha gijk}^{hom} / SE_{gijk} \quad (2.22)$$

$$D_{gijk}^{SE} = D_{gijk}^{hom} / SE_{gijk} \quad (2.23)$$

Now, the homogeneous nodal balance equation becomes

$$\begin{aligned} -D_{gijk}^{SE} \frac{d^2}{dx^2} \phi_{gijk}^{x,SE}(x) + \sum_i^{SE} \phi_{gijk}^{x,SE}(x) \\ - \sum_{g'=1}^G (\sum_{gg'ijk}^{SE} + \frac{1}{\lambda^{hom}} M_{gg'ijk}^{SE}) \phi_{gijk}^{x,SE}(x) \\ = -S_{gijk}^{y,z,SE}(x) \quad (2.24) \end{aligned}$$

where

$$S_{gijk}^{y,z,SE}(x) \equiv \frac{1}{h_y^j} L_{gijk}^{y,SE}(x) + \frac{1}{h_z^k} L_{gijk}^{z,SE}(x) \quad (2.25)$$

$$L_{gijk}^{y_j SE}(x) \equiv \frac{1}{h_z^k} \int_{y_j}^{y_{j+1}} dy \int_{z_k}^{z_{k+1}} dz \frac{\partial}{\partial y} J_{gijk}^{y_j SE}(r) \tag{2.26}$$

$$\bar{J}_{gijk}^{SE}(x) = -D_{gijk}^{SE} \frac{d}{dx} \phi_{gijk}^{SE}(x) \tag{2.27}$$

Then, the SE-flux solution of above equations is related to the equivalent flux solution by:

$$\phi_{gijk}^{SE}(x) = SE_{gijk}^x \phi_{gijk}^{hom}(x) \tag{2.28}$$

This SE-solution conserves the integral reaction and leakage rates, but not the integral fluxes. The discontinuity condition (2.21) can now be replaced the continuity condition:

$$\phi_{g_{i-1},j,k}^{SE}(x_i) = \phi_{g_{i,j,k}^{SE}}(x_i) \tag{2.29}$$

Similar to conventional cross-section libraries, the heterogeneity factor is no longer needed explicitly. This gives large benefit of using conventional diffusion code to calculate the homogenized global problem, compared with the nodal equivalent methods.

### III. Application of Homogenization Method

#### III.1. Introduction

Results of global-nodal problems are affected by the nodal homogenization theory and baffle treatment method, as well as by the calculational tool.

Nodal homogenization theory is treated in two approaches-approximate nodal equivalence method using AXS, ADF and simplified equivalence method using SE-library.

The usual strategy in nuclear industry for the presence of the core baffle and the reflector is to preclude these regions from the nodal calculation and to simulate their presence by the imposition of albedo conditions at the core boundaries. Obtaining the albedo values is very expensive and also cumbersome work to carry out. In this study, two other models are adopted hereinafter. One is the explicit baffle method in which the baffle region is modeled explicitly as nodes in the nodal solution. And the other

is the homogenized baffle method in which the baffle is smeared with reflector material by means of auxiliary calculations.

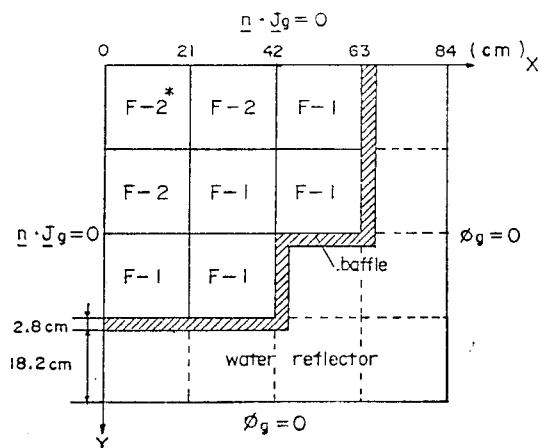
To perform the comparative study for various homogenization methods, a reference solution is required against which the accuracy of the nodal method results will be tested. For this purpose, fine-mesh heterogeneous calculation is carried out by KIDD<sup>2)</sup> with a two energy group model.

As a realistic, but not so complicated problem, EPRI-9 and EPRI-9R benchmark problems are tested.

#### III.2. The EPRI-9 Benchmark Problem

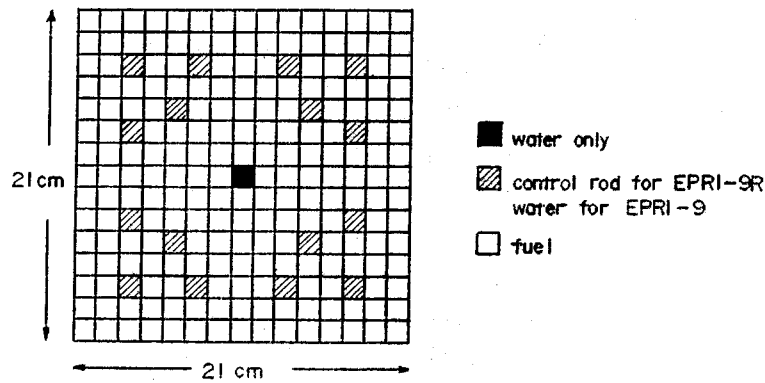
This problem depicted in Fig. 3-1, provides a fairly accurate representation of the peripheral regions of PWRs. The EPRI-9 problem has one-eighth-core symmetry, and unrodded fuel assemblies of two different enrichments are loaded in the core. The heterogeneous geometric detail of each assembly is shown in Fig. 3-2, and the cross-sectional data for the various material compositions are given in Table 3-1.

A rodded version of EPRI-9 problem, called the EPRI-9R problem, will also be used for benchmark calculations. In this problem, a control rod is inserted into the center assembly



\* F-2\* is unrodded fuel for EPRI-9 problem, but rodded fuel for EPRI-9R problem

Fig. 3-1. Quadratic Core Layout of the EPRI-9 and EPRI-9R Problem



Dimension of each cell=1.4cm by 1.4cm

Fig. 3-2. Heterogeneous PWR Assembly Geometry

Table 3-1. Heterogeneous, 2-Group Cross-section Data

Material	Group	$D_g$ (cm)	$\Sigma_{ag}$ (cm <sup>-1</sup> )	$\Sigma_R$ (cm <sup>-1</sup> )	$\nu\Sigma_{f_g}$ (cm <sup>-1</sup> )	$\kappa\Sigma_{f_g}$ (cm <sup>-1</sup> )
Fuel-1 (F-1)	1	1.500	0.0130	0.0200	0.0065	0.0026
	2	0.400	0.1800		0.2400	0.0960
Fuel-2 (F-2)	1	1.500	0.0100	0.0200	0.0050	0.0020
	2	0.400	0.1500		0.1800	0.0720
Water (W)	1	1.700	0.0010	0.0350	0.0	0.0
	2	0.350	0.0500		0.0	0.0
Baffle (B)	1	1.020	0.0032	0.0000	0.0	0.0
	2	0.335	0.1460		0.0	0.0
Control rod (CR)	1	1.113	0.0800	0.0038	0.0	0.0
	2	0.184	0.9600		0.0	0.0

in Fig. 3-1.

### III. 3. Homogenization of Fuel Assembly

The calculation of homogenized parameters for fuel assemblies is carried out for three unique fuel types of EPRI-9 problem-F-1, F-2, and F-2R assemblies. This is performed by a

finite difference method (KIDD) and analytic nodal method (ANM) as a local assembly calculation with  $n. Jg=0$  boundary.

Tables 3-2 and 3-3 show assembly homogenized cross-sections and SE parameters, respectively. AXS were calculated by KIDD fine

Table 3-2. Result of Assembly Homogenized Cross-sections Calculated by KIDD

Assembly	Group	$D_g$	$\Sigma_{ag}$	$\Sigma_R$	$\nu\Sigma_{f_g}$	$\kappa\Sigma_{f_g}$
F-1	1	1.5150	0.12098-1	0.21127-1	0.60117-2	0.24047-2
	2	0.39570	0.16882		0.21935	0.87741-1
F-2	1	1.5150	0.93242-2	0.21126-1	0.46245-2	0.18498-2
	2	0.39579	0.14157		0.16483	0.65934-1
F-2R	1	1.4742	0.41795-1	0.18949-1	0.46316-2	0.18526-2
	2	0.39048	0.18377		0.17114	0.68454-1

**Table 3-3. SE Parameters of Fuel Assemblies using Fine-Mesh Finite Difference Method**

Assembly	Group	SE
F-1	1	1.0029
	2	0.9304
F-2	1	1.0035
	2	0.9395
F-2R	1	1.0180
	2	1.1699

mesh heterogeneous assembly calculation, and SE parameters were calculated by Eq. 2. 20 from dividing the heterogeneous surface flux by the node average flux which is equal to homoge-

neous surface flux as done in Eqs. 2. 18 and 2. 19. Therefore we need no additional fine-mesh local calculation for homogenized assembly.

Notwithstanding the convenience of simplified equivalence theory, approximate nodal equivalence theory is more general and reliable approach. In this method, node AXSs are obtained by ANM, and ADFs are obtained by ANM code package<sup>7)</sup> (ANM-ANMED-ADF). These AXS and ADF can also be obtained by KIDD and its subsidiaries<sup>8)</sup> (KIDD-HOMOS-CALAXS) which are not theoretically consistent with global calculation tool-ANM. Computational results are shown in Table 3-4 and 3-5.

**Table 3-4. Results of AXS Calculated by ANM**

Assembly	Group	$D_g$	$\Sigma_{ag}$	$\Sigma_R$	$\nu\Sigma_{f_t}$	$\kappa\Sigma_{f_t}$
F-1	1	1.5150	0.12099-1	0.21126-1	0.60122-2	0.24049-2
	2	0.39559	0.16855		0.21885	0.87541-1
F-2	1	1.5150	0.93248-2	0.21125-1	0.46249-2	0.18500-2
	2	0.39571	0.14141		0.16454	0.65815-1
F-2R	1	1.4742	0.14788-1	0.18951-1	0.46323-2	0.18529-2
	2	0.39153	0.17981		0.17201	0.68805-1

**Table 3-5. Results of ADFs Calculated by ANM**

Assembly	Group	ADF	
		center	edge
F-1	1	1.0013	1.0030
	2	0.9695	0.9289
F-2	1	1.0014	1.0036
	2	0.9737	0.9384
F-2R	1	1.0165	1.0173
	2	1.1977	1.1574

**III. 4. Treatment of Baffle and Reflector**

A method for solving EPRI-9(and EPRI-9R) problem is to model the baffle explicitly as nodal regions in the ANM solution. The nodal mesh layout is shown in Fig. 3-3. The main drawback is the increase in the number of nodes by a factor approaching nine over calculation done

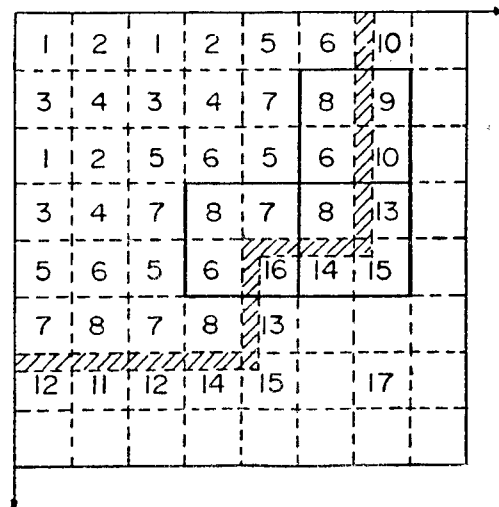


**Fig. 3-3. Core Nodal Mesh Layout for the EPRI-9 Problem Showing Three Unique Color-sets Consisting of Fuel, Baffle and Reflector**



**Table 3-6. Comparison of Discontinuity Factors Obtained from Two Homogenization Method—FDM and ANM for the baffle-Reflector Color-sets**

Node number	Group	Calculation Tool	ADF for surface			
			left	right	top	bottom
13	1	a *	1.0882	0.8323	0.9308	0.9275
		b *	1.1824	0.8798	1.0550	0.9270
	2	a	0.4953	1.5631	1.0872	0.8802
		b	0.3094	1.7138	1.0410	0.9525
16	1	a	1.0012	0.8536	1.0012	0.8536
		b	1.0916	0.9597	1.0916	0.9597
	2	a	0.5557	1.5394	0.5557	1.5394
		b	0.3411	1.5339	0.3411	1.5339

\* a : finite difference method using KIDD-HOMOS-CALAXS like as SE parameter calculation

b : analytic nodal method using ANM-ANMED-ADF

with assembly-sized nodes. This increase results from the necessary extension of the baffle mesh lines throughout the core and from the need for smaller nodes. Because of the large number of nodes, computer storage requirements are significantly increased when the calculation is performed for the realistic large power reactors.

An alternative to this problem is the application of the homogenized baffle method. The calculation of homogenized parameters (AXS and ADF) for baffle-reflector nodes poses some difficulty, because the usual method of homogenization cannot be applied to non-multiplying nodes. For this reason, baffle homogenization is performed by color-set homogenization method.

Color-sets are assembly-sized regions composed of four quadrants of different assemblies. Evaluation of the AXS and ADF (or SE) for baffle-reflector nodes are performed by these color-set local calculations with  $n.Jg=0$  boundary conditions. As shown in Fig. 3.3, necessary color sets for the EPRI-9 problem are three types.

As done in fuel assembly calculation, homogenization calculations for the color-sets were done by FDM (KIDD) and analytical nodal method (ANM). Color set ADFs were also calculated by these two methods, ANM code

package<sup>7)</sup> and KIDD code subsidiaries<sup>8)</sup>. Table 3-6 shows parts of the results of these two colorset ADF calculations for the problem in Fig. 3-3.

By the way, calculation of ADF using the finite difference method in Table 3-6 is not consistent with the global nodal method-ANM.

Since SE-parameters are assumed to be equal on the opposite surfaces, we must choose a value from the calculated four ADFs at each surface in order to use simplified equivalence

**Table 3-7. Calculation Method for SE-library Usage of Baffle-Reflector Nodes**

Calculation method #	Fuel node		Baffle and water node	
	AXS	SE	AXS	SE
C1	LFA	LFA	CS	Inter.
C2	LFA	LFA	CS	Avg.
C3	CS	Inter.	CS	Inter.
C4	CS	Avg.	CS	Inter.
C5	CS	Avg.	CS	Avg.

\* LFA : AXSs are obtained from local fuel assembly calculation.

CS : AXS are obtained from baffle-reflector color-set calculation

Inter. : SE Parameters are chosen as a fuel-baffle interface value

Avg. : SE parameters are calculated as an average value of four surface ADFs.

**Table 3-8. Summary of Global Computational Results from Five Methods Listed in Table 3-7.**

Calculation method#	% error in $K_{eff}$	% error in nodal power	
		Max. error	Avg. error
C1	-0.064	0.657	0.332
C2	-0.014	3.416	1.523
C3	0.100	5.436	2.498
C4	0.032	0.936	0.384
C5	0.074	3.531	1.561

theory. To establish an optimum SE-parameters for the baffle reflector color-set, five possible methods were tested.

As shown in Table 3-8, methods C1 and C4 turned out to be appropriate from the five possible methods. And method C1 is known to be the most desirable since method C4 needs ineffectual efforts considering the boundary fuel nodes by color-set. Therefore, color-set calculations are needed only for the generation of SE-library for baffle-reflector homogenized nodes. And SE-parameters for these nodes must be the value of the interesting surface, i.e., fuel-baffle inter-face.

**III.5. Result of the Global Calculation**

To testify the benefit of the simplified equivalence theory, a global reactor problem with

homogenized baffle boundary is solved by the fine mesh FDM and assembly sized nodal method. As shown in Figure 3-4, SE-library has stronger advantage to the relative nodal power over the conventional homogenized cross-section library regardless of global calculation tool. Therefore, we can visualize that the simplified equivalence theory is an excellent homogenization method. But this method does not have strict theoretical basis on the modeling of flux discontinuity and nodal surface currents. Analytic nodal method using AXS and ADF is a far advanced tool in this aspect. In this section, utility of ADF is compared with SE parameters.

Figure 3-5 shows results of nodal power and  $K_{eff}$  calculated by ANM, coarse-mesh nodal calculation for the explicit baffle problem with four nodes per assembly. As a result, the use of AXS/ADF (ANM package) does not yield better criticality and nodal power results than the use of SE-library (KIDD and its subsidiaries), but does than the use of AXS/UDF. However, even the use of UDF (unity discontinuity factors), i.e., conventional homogenization method, yields allowable results less than 0.66% error.

For problems in which baffle is homogenized

1.4444	1.2176	0.8480	
-1.724	-1.396	1.191	
0.222	-0.115	-0.318	
0.249	-0.107	-0.307	
	1.2067	0.6089	reference relative power
	-0.953	4.139	% error (a)
	-0.257	0.657	% error (b)
	-0.315	0.640	% error (c)

reference  $K_{eff}=0.928003$

% error (a)=0.064

(b)=-0.064

(c)=-0.062

average % error (a)=2.016

(b)=0.332

(c)=0.334

(a) KIDD fine-mesh FDM calculation using conventional homogenization method

(b) KIDD fine-mesh FDM calculation using SE-library

(c) ANM coarse mesh nodal calculation using SE-library

**Fig. 3-4. Nodal Power and  $K_{eff}$  Results Obtained by Color-set Baffle-Reflector Homogenization.**

0.65746	0.61707	0.52549	0.35695
-0.151	-0.310	-0.255	-0.630
-0.166	-0.326	-0.276	-0.658
0.192	0.058	0.158	0.112
0.179	0.045	0.139	0.073
0.239	0.105	0.204	0.146
1.08571	1.03159	0.89909	0.65412
0.040	-0.192	-0.271	-0.183
0.033	-0.201	-0.281	-0.203
0.115	-0.101	-0.174	0.228
0.111	-0.090	-0.175	0.220
0.157	-0.044	-0.121	0.283
1.15242	1.10346	1.21005	0.97447
0.220	0.128	-0.109	-0.039
0.228	0.135	-0.116	-0.050
0.019	-0.104	-0.050	0.071
0.013	-0.106	-0.017	0.099
-0.055	-0.177	0.034	0.154
1.33187	1.28247	1.43227	
0.169	0.127	-0.072	
0.182	0.139	-0.075	
-0.020	-0.094	-0.006	
-0.028	-0.097	0.023	
-0.083	-0.158	0.077	
1.44303	1.39446	reference relative power	
0.203	0.117	-(a) AXS (KIDD) UDF	
0.220	0.131	-(b) AXS (ANM), UDF	
-0.009	-0.086	-(c) SE-library (KIDD)	
-0.013	-0.087	-(d) AXS (KIDD), ADF (CALAXS)	
-0.062	-0.140	-(e) AXS (ANM), ADF (ADF)	
1.49722	reference $K_{eff}$ =0.928003		
0.285	% error (a)=-0.008		
0.304	(b)=-0.065		
0.061	(c)= 0.002		
0.055	(d)= 0.002		
0.009	(e)=-0.056		

average % error (a)=0.203  
 (b)=0.215  
 (c)=0.097  
 (d)=0.090  
 (e)=0.129

max. % error (a)=-0.630  
 (b)=-0.658  
 (c)= 0.228  
 (d)= 0.220  
 (e)= 0.283

Fig. 3-5. Nodal Power and  $K_{eff}$  Results Obtained by ANM Code for Explicit Baffle Problem of EPRI-9 Benchmark Problem

0.65746	0.61707	0.52549	0.35695
4.747	4.883	5.342	12.212
0.402	0.334	0.398	3.236
-0.715	-0.922	-1.178	-1.460
-0.691	-0.823	-0.748	-0.202
-0.748	-0.883	-0.811	-0.275
1.08571	1.03159	0.89909	0.65412
-1.012	-1.032	-0.483	4.901
-0.608	-0.806	-0.764	1.365
0.125	-0.134	-0.300	-1.261
0.050	-0.164	-0.197	-0.541
0.004	-0.210	-0.249	-0.602
1.15242	1.10346	1.21005	0.97447
-1.233	-1.174	-1.088	-0.149
-0.167	-0.319	-0.369	-0.438
0.246	0.063	0.113	0.061
0.146	-0.018	0.055	-0.277
0.214	0.053	0.003	-0.332
1.33187	1.28247	1.43227	
-1.539	-1.468	-1.479	
0.077	-0.054	0.136	
0.414	0.279	0.344	
0.294	0.167	0.242	
0.349	0.227	0.186	
1.44303	1.39446	reference relative power	
-1.665	-1.662	-(a) AXS (KIDD), UDF	
0.247	0.098	-(b) SE-library (KIDD)	
0.555	0.415	-(c) AXS (ANM), ADF (ADF)	
0.421	0.288	-(d) AXS (ANM), ADF (ADF)	
0.469	0.340	-(e) Hybrid method	
1.49722	reference $K_{eff}$ =0.928003		
-1.665	% error (a)= 0.063		
0.391	(b)=-0.062		
0.686	(c)=-0.106		
0.545	(d)=-0.101		
0.590	(e)=-0.043		

avg. % error (a)=2.829  
 (b)=0.605  
 (c)=0.532  
 (d)=0.324  
 (e)=0.364

max. % error (a)= 12.212  
 (b)= 3.236  
 (c)=-1.460  
 (d)=-0.823  
 (e)=-0.883

Fig. 3-6. Nodal Power and  $K_{eff}$  Results Obtained by ANM Code for Homogenized Baffle Problem of EPRI-9 Benchmark Problem

with reflector, the use of ADF is shown to be necessary. This is well exhibited in Figure 3-6. The maximum error in nodal power is reduced to -0.823%, from 12.212%, and the average error is to 0.324% from 2.829% by using ADF instead of UDF. And the use of ADF is better than the use of SE parameters contrary to the explicit baffle problem.

AXS and ADF of the fuel nodes at the baffle boundary were obtained by two ways; one was by baffle color-set calculation, method (c) in Fig. 3-6, the other was by fuel assembly local calculation, method (d).

Method (d) produces slightly better results than method (c). Therefore, to get the AXS and ADF for the boundary fuel nodes from the color-set is needlessly painstaking, because it requires more unique nodes than those of the method (d) shown in Fig. 3-3.

Table 3-9 is a summary of results obtained from the various ANM solution models for the EPRI-9 problem. On the aspects of criticality, analytic nodal method is less advantageous over the finite difference method as a homogenization tool.

When node homogenization is performed only for fuel assemblies, ADFs are simplified by Eqs. 2.18 and 2.19. Therefore, no additional calculation is required for homogenized node to solve the Equation 2.15. Since ANM code

packages use this equation, predicted ADFs may be different from the values obtained by KIDD assembly calculation using Equations 2.18 and 2.19. In the calculation of AXS, fine-mesh FDM (KIDD) calculation will be more reliable than the fine-mesh ANM (ANM) calculation which has some inherent assumption. Because of this reason, fuel assembly AXS and ADF calculated by ANM are predicted with some differences in assembly reactivity, and this leads to a worse prediction in criticality. This trend spreads to the nodal power prediction in the explicit baffle problem as shown in Table 3-9.

To verify this effect, method (e) in Figure 3-6 is tested. This method is a hybrid one in which fuel assembly homogenization is performed by finite difference method (KIDD-CALAXS).<sup>8)</sup> However the baffle-reflector homogenization is done inevitably by ANM-ADF<sup>7)</sup>. As shown in Fig. 3-6 and Table 3-9, this method gives a good result in prediction of both criticality and nodal powers even though this method does not keep the consistency between the homogenization and the global calculation.

This hybrid method has a greater benefit to the rodged problem as shown in Figure 3-7. By using this method, two troublesome regions are well homogenized. For the rodged assembly, analytic nodal method cannot carry out homog-

**Table 3-9. Summary of Criticality and Nodal Power Results by Salient ANM Solution Models for the EPRI-9 Problem**

Baffle Treatment	Homogenization Tool	Method	% error in $K_{eff}$	% error in nodal power	
				Max.	Avg.
Explicit Baffle	KIDD (UDF)	(a) in Fig. 3-7	-0.008	-0.630	0.203
	KIDD (SE)	(c) in Fig. 3-7	0.002	0.228	0.097
	KIDD-CALAXS	(d) in Fig. 3-7	0.002	0.220	0.090
	ANM-ADF	(e) in Fig. 3-7	0.056	0.283	0.129
Color-set Homogenized Baffle	KIDD (UDF)	(a) in Fig. 3-8	0.063	12.212	2.829
	KIDD (SE)	(b) in Fig. 3-8	-0.062	3.236	0.605
	ANM-ADF	(d) in Fig. 3-8	-0.101	-0.823	0.324
	KIDD-CALAXS & ANM-ADF	(e) in Fig. 3-8	-0.043	-0.883	0.364

0.86632	0.82698	0.72184	0.49913
5.042	4.949	5.476	12.474
0.912	0.619	0.738	3.640
-0.975	-1.377	-1.347	-0.868
-0.212	-0.579	-0.481	0.048
1.32385	1.29231	1.17373	0.88310
-1.226	-1.438	-0.717	4.975
-0.315	-0.736	-0.584	1.718
-0.094	-0.618	-0.709	-1.103
0.462	0.002	0.023	-0.283
1.19866	1.20924	1.43901	1.24740
-1.887	-1.985	-1.644	-0.394
-0.024	-0.401	-0.335	-0.253
0.430	-0.120	-0.321	-0.781
0.529	0.122	0.153	-0.104
1.02911	1.10542	1.47758	
-3.966	-3.791	-2.614	
0.004	-0.215	-0.317	
1.242	0.669	0.076	
0.330	0.117	0.122	
0.53988	0.66062	reference relative power	
-1.319	0.197	(a) AXS (KIDD), UDF	
-1.408	-1.399	(b) SE-library (KIDD)	
4.288	3.348	(c) AXS (ANM), ADF (ADF)	
-0.865	-0.721	(d) Hybrid method	
0.39726	reference $K_{eff}=0.889154$		
-2.960	% error (a)= 0.050		
-1.364	(b)=-0.126		
6.062	(c)=-0.059		
-0.992	(d)=-0.111		
	avg. % error (a)=3.373	max. % error (a)= 12.474	
	(b)=0.832	(b)= 3.640	
	(c)=1.206	(c)= 6.062	
	(d)=0.324	(d)=-0.992	

Fig. 3-7. Nodal Power and  $K_{eff}$  Results Obtained by ANM Code for Homogenized Baffle Problem of EPRI-9R Benchmark Problem

enization work well because of strong heterogeneity around the control rod nodes. Therefore this hybrid method is the only effective method to predict criticality and relative nodal powers within a proper error bounds.

Inadequacy of ANM for fuel assembly nodes is intensified by the computing time consumed, as shown in Table 3-10. But for the homogenized baffle problem, ANM package is indis-

pensable for calculating ADFs of the baffle-reflector homogenized nodes and for lessening the errors which may result from.

The use of homogenized color-set baffle treatment needs much more calculation and computing time than the explicit baffle treatment, but on the other hand it lessens the time for global calculation. This effect may make the homogenized baffle method more beneficial in

**Table 3-10. Summary of Computing Time Consumed by Salient ANM Solution Models for the EPRI-9 Problem** (Unit in Second)

Calculation Model	Fuel assembly node		Baffle & Water node		Global Calculation	Total	Method
	AXS*	DF**	AXS	DF			
Global Heterogeneous Fine-mesh FDM	—	—	—	—	KIDD 1800	1800	Reference
Conventional Homogenization	KIDD 66	—	—	—	ANM 23	89	(a) in Fig. 3-7
Explicit Baffle	KIDD 66	SE 2	—	—	ANM 11	79	(c) in Fig. 3-7
	KIDD 66	CALAXS 3	—	—	ANM 22	91	(d) in Fig. 3-7
	ANM 394	ADF 3	—	—	ANM 22	419	(e) in Fig. 3-7
Color-set Homogenized Baffle	KIDD 66	SE 2	KIDD 136	SE 146	ANM 6	356	(b) in Fig. 3-8
	ANM 394	ADF 3	ANM 557	ADF 4	ANM 11	969	(c) in Fig. 3-8
	KIDD 66	CALAXS 3	ANM 557	ADF 4	ANM 11	641	(e) in Fig. 3-8

\* AXS: Calculation for Assembly Homogenized Cross-sections

\*\* DF: Calculation for Discontinuity Factors

the large power reactor problem, in which assembly number is large but unique color-set number for baffle homogenization is finite even though baffle geometry is complex. The most reliable results are obtained from the hybrid method as shown in Figs. 3-6 and 3-7.

#### IV. Conclusion and Recommendation

The coarse-mesh nodal method has been shown to provide excellent predictions of criticality and nodal powers for PWRs. For 2-D, non-depleting unrodded benchmark problem (EPRI-9 problem), nodal powers were obtained within 0.8% error and  $K_{eff}$  within 0.1% error relative to the fine-mesh reference solution. The use of discontinuity factors (SE-parameters or ADF) in the ANM calculation was shown to be necessary for accurate prediction of nodal powers for problems in which the core baffle is not explicitly modeled by nodal regions.

Explicit baffle treatment gave an excellent result regardless of calculational tool and homogenization method. But this method needs larger computing expenses and memory requirement which limit the applicability for treating large

core problems. And this cannot assure the accurate prediction of surface average fluxes since discontinuity factors for baffle node must be unity. Therefore, this method induces unacceptable errors in detailed flux reconstruction calculation<sup>5)</sup>.

As an appropriate procedure for the nodal calculation, the following are recommended:

1. The core and reflector are divided into quarter assembly nodes.
2. 2-D, fine-mesh homogenization calculations are run with  $n \cdot J_g = 0$  boundary conditions for each type of fuel assembly. These calculations yield AXS and ADF for each quarter assembly node.
3. 2-D fine-mesh homogenization calculations are run for color-set regions in the core periphery to get the AXS and ADF for homogenized baffle-reflector nodes.
4. The ANM coarse-mesh nodal calculation is run to yield the global eigenvalue and node-average powers.

In the step 2, it is recommended that AXS and ADF be obtained by finite difference method instead of analytic nodal method. Finite difference method offers an accuracy and time saving

for homogenization without theoretical difficulty.

For the practical application for the realistic PWR problems, installation of depletion scheme and reconstruction scheme is requisite. Evaluations and applications of the depletion procedures and the flux reconstruction (dehomogenization) are studied at present, and will be presented in a foreseeable future.

### References

1. J. Chang, K.S. Moon and M.H. Kim, "ANM; Coarse-mesh Nodal Code based on Analytic Nodal Method", KAERI (to be published).
2. S.K. Lee, K.S. Moon, J. Chang and B.J. Jun, "KIDD, A KAERI Improved Diffusion Depletion Program for Nuclear Reactor Analysis", KAERI (to be published).
3. K. Koebke, "Advances in Homogenization and Dehomogenization", Topical Meeting on Advances in Mathematical Methods for the Solution of Nuclear Engineering Problems, München, F.R.G., April 1981.
4. K.S. Smith, "Spatial Homogenization Methods for Light Water Reactor Analysis", Ph. D. Thesis, M.I.T., Cambridge, MA, June 1980.
5. H.S. Khalil, "The Application of Nodal Methods to PWR Analysis", Ph. D. Thesis, M.I.T., Cambridge, MA. Jan. 1983.
6. C.L. Hoxie, "Application of Nodal Equivalence Theory to the Neutronic Analysis of PWRs", Ph. D. Thesis, M.I.T., Cambridge, MA, June 1982.
7. J. Chang, "ADF, A Code Package for Calculation of Discontinuity Factors based on Analytic Nodal Method", KAERI (to be published).
8. M.H. Kim, "CALAXS, A Program Package for Calculation of Homogenization Parameters", KAERI (to be published).